crystals

MDPI

Article

Contrasting Coordination- and Debromination-Driven Dimerization of Dibenzo[c,g]carbazole Derivatives on Ag(111) Visualized by STM

Yan Li [1], Xiang Zhang [2], Maoyun Lang [2], Shenwei Chen [2,3] and Peng Hu [2,*]

[1] Huayou New Energy Technology (Quzhou) Co., Ltd., Quzhou 324012, China
[2] State Key Laboratory of Green Chemical Synthesis and Conversion, College of Chemical Engineering, Zhejiang University of Technology, Hangzhou 310014, China; csw@zjut.edu.cn (S.C.)
[3] School of Chemistry, Sun Yat-sen University, Guangzhou 510275, China
* Correspondence: hupchem@zjut.edu.cn

Abstract

Here, we report a comparative scanning tunneling microscopy study of two brominated dibenzo[c,g]carbazole derivatives on Ag(111): 5,9-dibromo-7H-dibenzo[c,g]carbazole (DBC) and 5,9,7-tribromo-7-(4-bromobutyl)-7H-dibenzo[c,g]carbazole (BrBu-DBC). At room temperature (RT), DBC forms ordered paired-row supramolecular assemblies, whereas annealing to 470 K induces the formation of butterfly-like dimers that further organize into periodic arrays, consistent with adatom-mediated N–Ag–N coordination. In contrast, BrBu-DBC shows disordered adsorption at RT but transforms at 490 K into dumbbell-shaped dimers coupled selectively at the terminal side chains, consistent with C–C linkage formation. We demonstrate how subtle functional modification modulates the competition between supramolecular assembly and surface-mediated transformation pathways.

Keywords: scanning tunneling microscopy; coordination assembly; debromination; carbazole derivatives; hierarchical self-assembly

1. Introduction

Single-crystal metal surfaces such as Au(111), Ag(111), and Cu(111) have emerged as versatile platforms for surface-confined crystallization, supramolecular engineering, and low-dimensional molecular construction [1–4]. Beyond serving as inert supports, these substrates can actively participate in interfacial chemistry: surface atoms and mobile adatoms may mediate coordination interactions, catalyze bond cleavage and formation, and thereby steer the transformation of molecular precursors into well-defined products [5–8]. This concept has enabled the development of on-surface synthesis, where target nanostructures—including graphene nanoribbons and porous covalent frameworks—can be generated with atomic precision while their reaction pathways are directly interrogated at the solid–vacuum interface [9].

Among the available characterization techniques, scanning tunneling microscopy (STM) plays a particularly important role, as it provides real-space access to molecular adsorption geometries, self-assembled phases, and thermally induced structural evolution with submolecular resolution [10–18]. Halogenated aromatic molecules have been widely employed as precursors in such studies, since C–X bond activation may give rise to covalent coupling, organometallic intermediates, or extended coordination networks [19–25]. Importantly, in addition to debromination-driven reaction routes, surface adatoms can

Check for updates

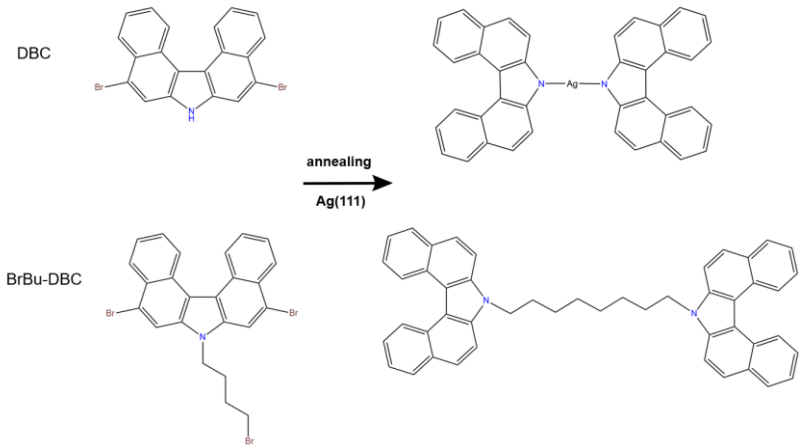
Academic Editor: Waldemar Maniukiewicz

Received: 24 February 2026
Revised: 22 March 2026
Accepted: 30 March 2026
Published: 8 April 2026

Copyright: © 2026 by the authors. Licensee MDPI, Basel, Switzerland. This article is an open access article distributed under the terms and conditions of the Creative Commons Attribution (CC BY) license.

serve as coordination nodes that stabilize metal–ligand motifs, offering an alternative building principle for two-dimensional crystalline assemblies [6,8,26]. Understanding how subtle variations in molecular functionalization determine the competition between these distinct pathways remains a central challenge for the rational design of surface-supported molecular crystals [27–29].

In this work, we investigate two closely related dibenzo[c,g]carbazole derivatives adsorbed on Ag(111): 5,9-dibromo-7H-dibenzo[c,g]carbazole (DBC) and 5,9,7-tribromo-7-(4-bromobutyl)-7H-dibenzo[c,g]carbazole (BrBu-DBC) (Scheme 1). Although both molecules share the same carbazole backbone, BrBu-DBC contains an additional flexible bromobutyl substituent, introducing a distinct functional site compared to the purely aryl-brominated DBC. By combining STM imaging with controlled thermal activation, we explore how such subtle structural modification influences the balance between supramolecular organization and surface-mediated transformation pathways [6,7]. The comparative nature of this study provides mechanistic insight into how coordination interactions and halogen-triggered processes can be selectively accessed on metal surfaces [30–32], offering guidance for the rational design of dimer-based building blocks and hierarchical molecular architectures at the interface [33,34].



Scheme 1. Schematic illustration of the surface-mediated assembly and dimerization pathways of DBC and BrBu-DBC on Ag(111).

2. Materials and Methods

All the STM experiments were performed at 78 K with a commercial Createc LT-STM (Createc Fischer & Co. GmbH, Erlangen, Germany). The base pressure was better than 1.0×10^{-10} mbar. The tip used in the experiment was a tungsten tip, which was electrochemically etched in 3 mol/L NaOH solution. STM images were taken in constant-current mode and all scanning probe images were edited using WSxM software (version 5.0 Develop 10.3) [35]. Atomically clean Ag(111) (from MaTecK GmbH, Jülich, Germany) was prepared through repeated cycles of argon ion (Ar+) bombardment (0.8 kV for 20 min) and annealing (750 K for 20 min). The DBC and BrBu-DBC molecules were synthesized in-house following previously reported procedures [36] and thermally sublimated onto the Ag(111) surface under a vacuum of ~3×10^{-9} mbar using a commercial molecular evaporator (Createc OLED-40-1-HL-WKCC-SHP, Createc Fischer & Co. GmbH, Erlangen, Germany).

3. Results and Discussion

DBC molecules were thermally deposited onto the Ag(111) surface at room temperature (RT), leading to the formation of well-defined ordered molecular islands (Figure 1a). Individual DBC molecules exhibit a characteristic V-shaped appearance with an anisotropic

contrast distribution. This distinct molecular signature is consistent with the geometry of the DBC backbone and is further supported by STM measurements of isolated DBC molecules on Cu(111), where single adsorbates can be stabilized and display a similar V-like topographic feature (Figure 1b). Within the ordered adlayers on Ag(111), the V-shaped DBC molecules preferentially align side by side along a common direction, indicating an anisotropic intermolecular packing motif on the substrate. High-resolution STM imaging (Figure 1c) further reveals that the molecular arrangement is highly directional: molecules within the same row adopt an identical orientation, whereas neighboring rows display an alternating contrast, suggesting an antiparallel alignment between adjacent molecular rows. Notably, the assembly exhibits a pronounced paired-row feature, in which two molecular rows associate as a coupled unit, giving rise to a distinct double-row packing motif across the adlayer, as highlighted by the white lines. Based on these observations, a structural model is proposed in Figure 1d. Within each molecular row, the linear arrangement is tentatively stabilized by directional halogen bonding interactions involving the brominated sites [37–40]. The measured intermolecular Br···Br separation of approximately 3.1 Å is consistent with typical halogen-bonding distances, supporting the role of such interactions in promoting one-dimensional ordering along the row direction [39,41]. In addition, the characteristic pairing of two adjacent rows can be attributed to complementary N···H–N interactions between neighboring carbazole units. The extracted N···N distance of about 3.0 Å falls within the characteristic range of hydrogen-bond-like interactions, indicating an effective inter-row stabilization mechanism.

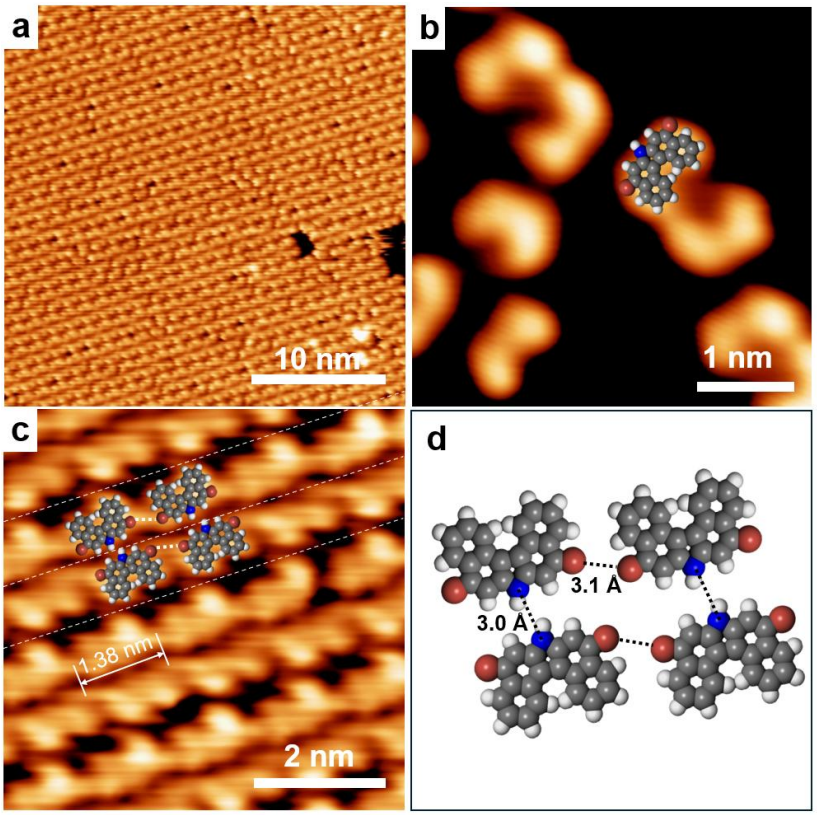


Figure 1. Supramolecular assembly of DBC at RT. (**a**) Large-scale STM image showing ordered molecular islands of DBC on Ag(111). (**b**) STM image of isolated DBC molecules on Cu(111). (**c**) High-resolution STM image revealing the directional paired-row packing motif with antiparallel alignment between adjacent rows. (**d**) Proposed structural model of the double-row assembly. White, brown, gray, and blue balls represent hydrogen, bromine, carbon, and nitrogen atoms, respectively. (**a**) *Vs* = −1.0 V, *It* = 100 pA. (**b**) *Vs* = −0.6 V, *It* = 100 pA. (**c**) *Vs* = −0.8 V, *It* = 100 pA.

In contrast, BrBu-DBC exhibits markedly different adsorption behavior at RT. As shown in Figure 2, no extended long-range ordered domains are observed; instead, the molecules form disordered aggregates without a well-defined periodic packing motif. This lack of structural regularity is likely related to the presence of the flexible bromobutyl substituent, which introduces additional conformational degrees of freedom and steric variability upon adsorption [42,43]. The alkyl side chain can adopt multiple conformations on the surface, leading to heterogeneous adsorption geometries and reducing the ability of the molecules to pack in a uniform manner. Moreover, the increased steric flexibility may weaken or disrupt directional intermolecular interactions, such as halogen bonding or other anisotropic interactions, which are essential for stabilizing ordered supramolecular assemblies [6]. These results suggest that even minor functional modifications, such as the introduction of a flexible alkyl bromine, can significantly alter the balance between molecular packing constraints and surface-confined crystallization at the interface.

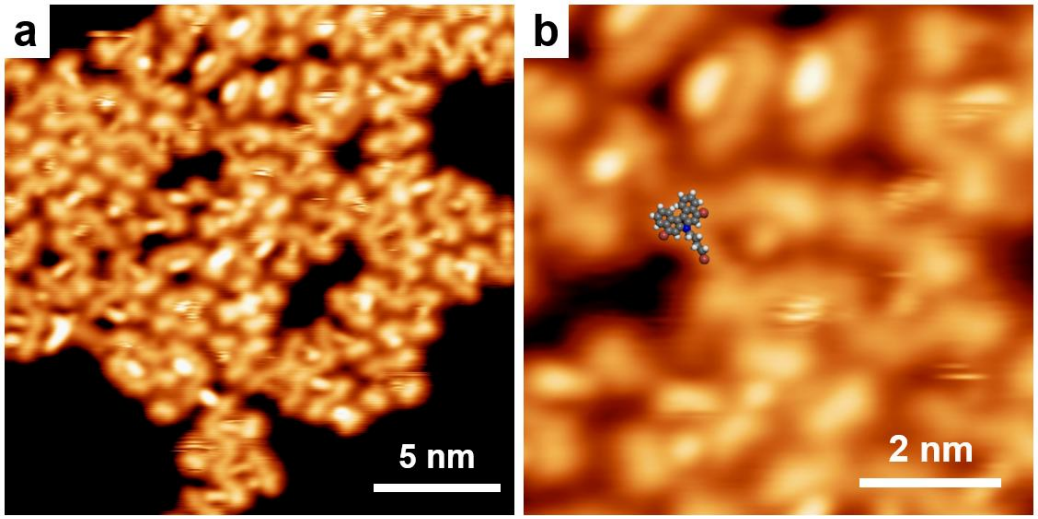


Figure 2. Adsorption behavior of BrBu-DBC on Ag(111) at RT. (**a**) Large-area STM image showing the absence of long-range ordered domains and the formation of disordered aggregates. (**b**) High-resolution STM image of a representative local region. White, brown, gray, and blue balls represent hydrogen, bromine, carbon, and nitrogen atoms, respectively. (**a**) $Vs = -2.0$ V, $It = 100$ pA. (**b**) $Vs = 1.0$ V, $It = 100$ pA.

As shown in Figure 3a, annealing the DBC/Ag(111) sample to 470 K induces a pronounced structural transformation accompanied by significant dimerization and reorganization of the molecular adlayer. Compared to the RT phase, the previously observed paired-row feature disappears completely, indicating that the initial supramolecular packing motif is no longer preserved upon thermal activation. High-resolution STM imaging (Figure 3b) reveals the emergence of a new dominant building block with a characteristic butterfly-like appearance. Hereafter, this motif is referred to as the butterfly dimer (BD). The formation of such dimers suggests that thermal annealing activates additional surface-mediated interactions beyond the weak halogen- and hydrogen-bonding contacts responsible for the RT assembly. In halogenated aromatic systems on coinage metal surfaces, annealing is often associated with C–Br bond activation and the disruption of halogen-bond-stabilized motifs, thereby enabling the development of new organometallic or coordination structures [19]. Accordingly, the disappearance of the linear row arrangement in the present system is consistent with a thermally driven reorganization process. Interestingly, the resulting adlayer exhibits a higher degree of hierarchical ordering. Specifically, two parallel molecular rows are periodically separated by an intercalated row of vertically oriented butterfly dimers, giving rise to an anisotropic stripe-like superstructure. The corresponding unit cell parameters

are measured to be approximately a_1 = 2.09 nm and b_1 = 4.16 nm, with an enclosed angle of θ_1 = 74°, as indicated in Figure 3b. Moreover, the characteristic central-node feature of the butterfly dimers suggests the involvement of surface adatoms [8,30]. Based on the structural dimensions and the presence of nitrogen coordination sites within the carbazole units, we tentatively attribute the linkage within the dimers to an adatom-mediated N–Ag–N coordination motif [44]. In this scenario, Ag adatoms serve as coordination nodes bridging two molecular backbones (Figure 3c). Notably, no extended C–C coupling products are observed for DBC before annealing at elevated temperatures causes molecular desorption from the surface. This indicates that coordination interactions in this system are kinetically more favorable than full debromination-driven C–C coupling, thereby dominating the reaction pathway at moderate temperatures [45]. For comparison, BrBu-DBC exhibits a markedly different thermally induced transformation behavior. As shown in Figure 3d, annealing the BrBu-DBC/Ag(111) system to 490 K results in the formation of well-defined dumbbell-shaped dimers that further organize into an ordered supramolecular lattice. The assembled phase is characterized by unit cell parameters of a_2 = 2.94 nm, b_2 = 1.35 nm, and an included angle of 56°, indicating a highly regular packing arrangement of the coupled species. High-resolution STM images (Figure 3e) demonstrate that two BrBu-DBC molecules are connected through their terminal side chains, with a measured center-to-center distance of approximately 1.8 nm. This structural feature strongly indicates that dimerization occurs selectively at the bromobutyl substituents rather than at the aromatic core. Therefore, these dumbbell dimers are tentatively attributed to a direct C–C coupling motif formed via debromination of the alkyl bromine followed by covalent carbon–carbon bond formation. The structural model overlaid in Figure 3e further supports this assignment, as the experimentally observed intermolecular separation is consistent with a direct C–C linkage between the terminal carbon sites. Notably, small protrusions highlighted by circles in Figure 3e are frequently observed in the inter-dimer regions. These features are attributed to residual bromine atoms remaining on the surface after C–Br bond cleavage [46]. During annealing, homolytic scission of the C–Br bonds generates surface-stabilized carbon species that subsequently undergo C–C coupling, while the liberated Br atoms are adsorbed on the Ag(111) surface. Such residual halogen species are commonly observed in on-surface Ullmann-type reactions and are consistent with the presence of debromination as the initiating step [47–49]. Additional support for the covalent nature of the junction is provided by bias-dependent STM measurements (Figure 3f). Upon varying the sample bias, the contrast at the junction evolves coherently with the molecular backbone rather than displaying a localized metallic-like feature, consistent with a delocalized electronic structure characteristic of a covalent C–C bond [47]. Together, these observations confirm that thermally induced debromination of the bromobutyl substituents leads to selective C–C bond formation and the subsequent emergence of an ordered dimeric assembly on Ag(111) [50]. Unlike DBC, where coordination stabilizes the reactive centers before full covalent coupling can occur, BrBu-DBC undergoes direct debromination and irreversible C–C bond formation at the flexible side chain.

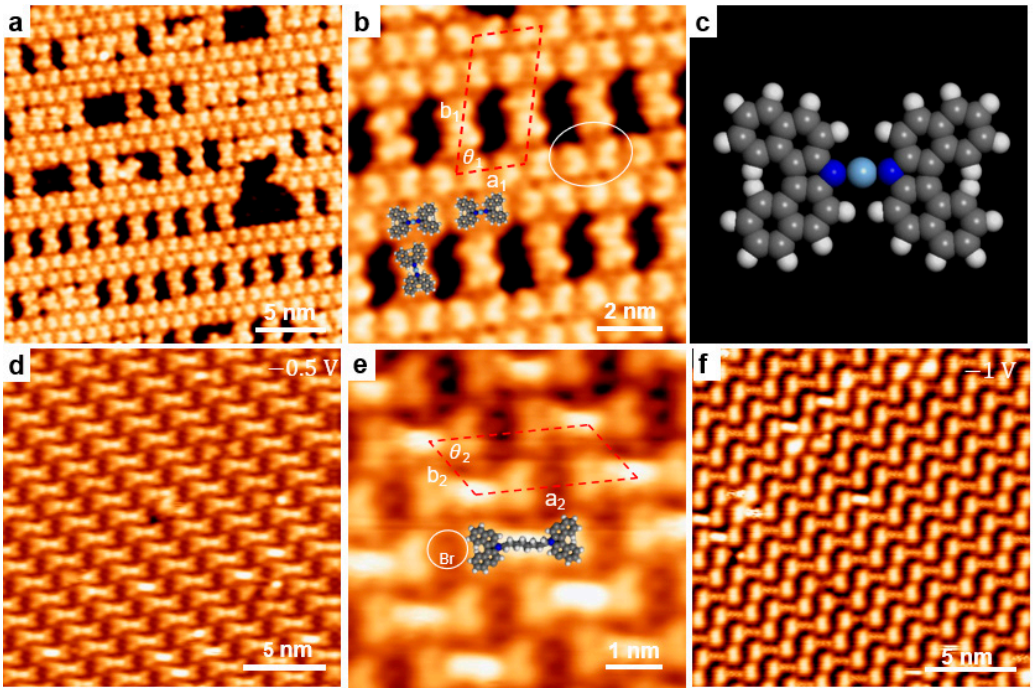


Figure 3. Thermally induced dimerization of DBC and BrBu-DBC on Ag(111). (**a**) Large-scale STM image of DBC after annealing to 200 °C. (**b**) High-resolution STM image of butterfly dimers; the unit cell parameters are a_1 = 2.09 nm, b_1 = 4.16 nm, θ_1 = 74°. (**c**) Proposed structural model of the BD motif. (**d**) Large-scale STM image of BrBu-DBC after annealing to 490 K. (**e**) High-resolution STM image of the dumbbell dimer. Circled bright protrusions are attributed to residual Br atoms remaining on the surface after debromination. (**f**) STM image of BrBu-DBC dumbbell dimers at different bias. White, cyan, gray, and blue balls represent hydrogen, silver, carbon, and nitrogen atoms, respectively. (**a**) *Vs* = −2.0 V, *It* = 100 pA. (**b**) *Vs* = −0.8 V, *It* = 100 pA. (**d**) *Vs* = −2.0 V, *It* = 100 pA. (**e**) *Vs* = −0.6 V, *It* = 100 pA. (**f**) *Vs* = −1.0 V, *It* = 100 pA.

4. Conclusions

We have investigated the self-assembly and dimerization behavior of DBC and BrBu-DBC on Ag(111) by STM. DBC forms ordered paired-row structures at RT and evolves into butterfly-like dimers upon annealing at 470 K, likely stabilized by adatom-mediated N–Ag–N coordination, followed by higher-order organization. In contrast, the introduction of a flexible bromobutyl substituent in BrBu-DBC selectively redirects the surface reaction pathway, enabling low-temperature side-chain dimerization at 490 K, consistent with C–C coupling. Overall, this study highlights how minor functional substitution controls competing coordination and debromination pathways on metal surfaces, enabling distinct dimer building blocks and hierarchical molecular assemblies.

Author Contributions: Conceptualization, S.C. and P.H.; methodology, X.Z. and S.C.; software, X.Z.; data curation, Y.L.; writing—original draft preparation, S.C., Y.L. and X.Z.; writing—review and editing, all authors; visualization, Y.L. and M.L.; supervision, P.H.; funding acquisition, S.C. and P.H. All authors have read and agreed to the published version of the manuscript.

Funding: This work was financially supported by the National Natural Science Foundation of China (No. 22308318, No. 22408330), the Zhejiang Provincial Natural Science Foundation of China (No. LQN25A040005, No. LQN25B060001, No. LD25B060004), and China Postdoctoral Science Foundation (No. 2025M771137).

Data Availability Statement: The original contributions presented in this study are included in the article. Further inquiries can be directed to the corresponding authors.

Acknowledgments: We thank the National Natural Science Foundation of China (No. 22308318, No. 22408330), Zhejiang Provincial Natural Science Foundation of China (No. LQN25A040005, No. LQN25B060001, No. LD25B060004), and China Postdoctoral Science Foundation (No. 2025M771137).

Conflicts of Interest: Author Yan Li was employed by the company Huayou New Energy Technology (Quzhou) Co., Ltd. The remaining authors declare that the research was conducted in the absence of any commercial or financial relationships that could be construed as a potential conflict of interest.

Abbreviations

The following abbreviations are used in this manuscript:

DBC	5,9-dibromo-7H-dibenzo[c,g]carbazole
BrBu-DBC	5,9,7-tribromo-7-(4-bromobutyl)-7H-dibenzo[c,g]carbazole
RT	Room temperature
STM	Scanning tunneling microscopy

References

1. Barth, J.V.; Costantini, G.; Kern, K. Engineering atomic and molecular nanostructures at surfaces. *Nature* **2005**, *437*, 671–679. [CrossRef] [PubMed]
2. Elemans, J.A.A.W.; Lei, S.; De Feyter, S. Molecular and Supramolecular Networks on Surfaces: From Two-Dimensional Crystal Engineering to Reactivity. *Angew. Chem. Int. Ed.* **2009**, *48*, 7298–7332. [CrossRef] [PubMed]
3. Kühnle, A. Self-assembly of organic molecules at metal surfaces. *Curr. Opin. Colloid Interface Sci.* **2009**, *14*, 157–168. [CrossRef]
4. Bartels, L. Tailoring molecular layers at metal surfaces. *Nat. Chem.* **2010**, *2*, 87–95. [CrossRef] [PubMed]
5. Gutzler, R.; Cardenas, L.; Rosei, F. Kinetics and thermodynamics in surface-confined molecular self-assembly. *Chem. Sci.* **2011**, *2*, 2290–2300. [CrossRef]
6. Dong, L.; Gao, Z.A.; Lin, N. Self-assembly of metal–organic coordination structures on surfaces. *Prog. Surf. Sci.* **2016**, *91*, 101–135. [CrossRef]
7. Clair, S.; de Oteyza, D.G. Controlling a Chemical Coupling Reaction on a Surface: Tools and Strategies for On-Surface Synthesis. *Chem. Rev.* **2019**, *119*, 4717–4776. [CrossRef]
8. Grill, L.; Hecht, S. Covalent on-surface polymerization. *Nat. Chem.* **2020**, *12*, 115–130. [CrossRef]
9. Palma, C.-A.; Samorì, P. Blueprinting macromolecular electronics. *Nat. Chem.* **2011**, *3*, 431–436. [CrossRef]
10. Binnig, G.; Rohrer, H. Scanning tunneling microscopy—From birth to adolescence. *Rev. Mod. Phys.* **1987**, *59*, 615–625. [CrossRef]
11. Eigler, D.M.; Schweizer, E.K. Positioning single atoms with a scanning tunnelling microscope. *Nature* **1990**, *344*, 524–526. [CrossRef]
12. Gimzewski, J.K.; Joachim, C. Nanoscale Science of Single Molecules Using Local Probes. *Science* **1999**, *283*, 1683–1688. [CrossRef] [PubMed]
13. Hla, S.-W.; Bartels, L.; Meyer, G.; Rieder, K.-H. Inducing All Steps of a Chemical Reaction with the Scanning Tunneling Microscope Tip: Towards Single Molecule Engineering. *Phys. Rev. Lett.* **2000**, *85*, 2777–2780. [CrossRef] [PubMed]
14. Weiss, P.S. Functional Molecules and Assemblies in Controlled Environments: Formation and Measurements. *Acc. Chem. Res.* **2008**, *41*, 1772–1781. [CrossRef]
15. Besenbacher, F.; Lauritsen, J.V.; Linderoth, T.R.; Lægsgaard, E.; Vang, R.T.; Wendt, S. Atomic-scale surface science phenomena studied by scanning tunneling microscopy. *Surf. Sci.* **2009**, *603*, 1315–1327. [CrossRef]
16. Gross, L. Recent advances in submolecular resolution with scanning probe microscopy. *Nat. Chem.* **2011**, *3*, 273–278. [CrossRef]
17. Xie, C.; Wu, Q.-M.; Li, R.-N.; Gu, G.-C.; Zhang, X.; Li, N.; Berndt, R.; Kröger, J.; Shen, Z.-Y.; Hou, S.-M.; et al. Isolated supramolecules on surfaces studied with scanning tunneling microscopy. *Chin. Chem. Lett.* **2016**, *27*, 807–812. [CrossRef]
18. Salmeron, M.; Eren, B. High-Pressure Scanning Tunneling Microscopy. *Chem. Rev.* **2021**, *121*, 962–1006. [CrossRef]
19. Zhong, D.; Franke, J.-H.; Podiyanachari, S.K.; Blömker, T.; Zhang, H.; Kehr, G.; Erker, G.; Fuchs, H.; Chi, L. Linear Alkane Polymerization on a Gold Surface. *Science* **2011**, *334*, 213–216. [CrossRef]
20. Méndez, J.; López, M.F.; Martín-Gago, J.A. On-surface synthesis of cyclic organic molecules. *Chem. Soc. Rev.* **2011**, *40*, 4578–4590. [CrossRef]
21. Fan, Q.; Wang, C.; Han, Y.; Zhu, J.; Hieringer, W.; Kuttner, J.; Hilt, G.; Gottfried, J.M. Surface-Assisted Organic Synthesis of Hyperbenzene Nanotroughs. *Angew. Chem. Int. Ed.* **2013**, *52*, 4668–4672. [CrossRef]
22. Sun, Q.; Zhang, C.; Li, Z.; Kong, H.; Tan, Q.; Hu, A.; Xu, W. On-Surface Formation of One-Dimensional Polyphenylene through Bergman Cyclization. *J. Am. Chem. Soc.* **2013**, *135*, 8448–8451. [CrossRef]

23. Zhou, X.; Wang, C.; Zhang, Y.; Cheng, F.; He, Y.; Shen, Q.; Shang, J.; Shao, X.; Ji, W.; Chen, W.; et al. Steering Surface Reaction Dynamics with a Self-Assembly Strategy: Ullmann Coupling on Metal Surfaces. *Angew. Chem. Int. Ed.* **2017**, *56*, 12852–12856. [CrossRef] [PubMed]
24. Lackinger, M. Surface-assisted Ullmann coupling. *Chem. Commun.* **2017**, *53*, 7872–7885. [CrossRef] [PubMed]
25. Yang, B.; Dong, B.; Chi, L. On-Surface Intramolecular Reactions. *ACS Nano* **2020**, *14*, 6376–6382. [CrossRef] [PubMed]
26. Ruffieux, P.; Wang, S.; Yang, B.; Sánchez-Sánchez, C.; Liu, J.; Dienel, T.; Talirz, L.; Shinde, P.; Pignedoli, C.A.; Passerone, D.; et al. On-surface synthesis of graphene nanoribbons with zigzag edge topology. *Nature* **2016**, *531*, 489–492. [CrossRef]
27. Lackinger, M. On the utility of complementary analytics for on-surface synthesis. *Nanoscale Horiz.* **2025**, *10*, 2172–2183. [CrossRef]
28. Barth, J.V. Molecular Architectonic on Metal Surfaces. *Annu. Rev. Phys. Chem.* **2007**, *58*, 375–407. [CrossRef]
29. Raval, R. Molecular assembly at surfaces: Progress and challenges. *Faraday Discuss* **2017**, *204*, 9–33. [CrossRef]
30. Stepanow, S.; Lingenfelder, M.; Dmitriev, A.; Spillmann, H.; Delvigne, E.; Lin, N.; Deng, X.; Cai, C.; Barth, J.V.; Kern, K. Steering molecular organization and host–guest interactions using two-dimensional nanoporous coordination systems. *Nat. Mater.* **2004**, *3*, 229–233. [CrossRef]
31. De Oteyza, D.G.; Gorman, P.; Chen, Y.-C.; Wickenburg, S.; Riss, A.; Mowbray, D.J.; Etkin, G.; Pedramrazi, Z.; Tsai, H.-Z.; Rubio, A.; et al. Direct Imaging of Covalent Bond Structure in Single-Molecule Chemical Reactions. *Science* **2013**, *340*, 1434–1437. [CrossRef] [PubMed]
32. Peyrot, D.; Silly, F. On-Surface Synthesis of Two-Dimensional Covalent Organic Structures versus Halogen-Bonded Self-Assembly: Competing Formation of Organic Nanoarchitectures. *ACS Nano* **2016**, *10*, 5490–5498. [CrossRef] [PubMed]
33. Cai, J.; Ruffieux, P.; Jaafar, R.; Bieri, M.; Braun, T.; Blankenburg, S.; Muoth, M.; Seitsonen, A.P.; Saleh, M.; Feng, X.; et al. Atomically precise bottom-up fabrication of graphene nanoribbons. *Nature* **2010**, *466*, 470–473. [CrossRef] [PubMed]
34. Lafferentz, L.; Eberhardt, V.; Dri, C.; Africh, C.; Comelli, G.; Esch, F.; Hecht, S.; Grill, L. Controlling on-surface polymerization by hierarchical and substrate-directed growth. *Nat. Chem.* **2012**, *4*, 215–220. [CrossRef]
35. Horcas, I.; Fernández, R.; Gómez-Rodríguez, J.M.; Colchero, J.; Gómez-Herrero, J.; Baro, A.M. WSXM: A Software for Scanning Probe Microscopy and a Tool for Nanotechnology. *Rev. Sci. Instrum.* **2007**, *78*, 013705. [CrossRef]
36. Wang, W.; Lin, Z.; Gao, S.; Zhu, W.; Song, X.; Tang, W. Versatile Self-Assembled Hole Transport Monolayer Enables Facile Processing Organic Solar Cells over 18% Efficiency with Good Generality. *Adv. Funct. Mater.* **2023**, *33*, 2303653. [CrossRef]
37. Aakeröy, C.B.; Fasulo, M.; Schultheiss, N.; Desper, J.; Moore, C. Structural Competition between Hydrogen Bonds and Halogen Bonds. *J. Am. Chem. Soc.* **2007**, *129*, 13772–13773. [CrossRef]
38. Metrangolo, P.; Meyer, F.; Pilati, T.; Resnati, G.; Terraneo, G. Halogen Bonding in Supramolecular Chemistry. *Angew. Chem. Int. Ed.* **2008**, *47*, 6114–6127. [CrossRef]
39. Cavallo, G.; Metrangolo, P.; Milani, R.; Pilati, T.; Priimagi, A.; Resnati, G.; Terraneo, G. The Halogen Bond. *Chem. Rev.* **2016**, *116*, 2478–2601. [CrossRef]
40. Talirz, L.; Söde, H.; Dumslaff, T.; Wang, S.; Sanchez-Valencia, J.R.; Liu, J.; Shinde, P.; Pignedoli, C.A.; Liang, L.; Meunier, V.; et al. On-Surface Synthesis and Characterization of 9-Atom Wide Armchair Graphene Nanoribbons. *ACS Nano* **2017**, *11*, 1380–1388. [CrossRef]
41. Fourmigué, M. Halogen bonding: Recent advances. *Curr. Opin. Solid State Mater. Sci.* **2009**, *13*, 36–45. [CrossRef]
42. Gao, H.-Y.; Wagner, H.; Zhong, D.; Franke, J.-H.; Studer, A.; Fuchs, H. Glaser Coupling at Metal Surfaces. *Angew. Chem. Int. Ed.* **2013**, *52*, 4024–4028. [CrossRef] [PubMed]
43. Pavliček, N.; Schuler, B.; Collazos, S.; Moll, N.; Pérez, D.; Guitián, E.; Meyer, G.; Peña, D.; Gross, L. On-surface generation and imaging of arynes by atomic force microscopy. *Nat. Chem.* **2015**, *7*, 623–628. [CrossRef] [PubMed]
44. Classen, T.; Fratesi, G.; Costantini, G.; Fabris, S.; Stadler, F.L.; Kim, C.; de Gironcoli, S.; Baroni, S.; Kern, K. Templated Growth of Metal–Organic Coordination Chains at Surfaces. *Angew. Chem. Int. Ed.* **2005**, *44*, 6142–6145. [CrossRef]
45. Bieri, M.; Treier, M.; Cai, J.; Aït-Mansour, K.; Ruffieux, P.; Gröning, O.; Gröning, P.; Kastler, M.; Rieger, R.; Feng, X.; et al. Porous graphenes: Two-dimensional polymer synthesis with atomic precision. *Chem. Commun.* **2009**, 6919–6921. [CrossRef]
46. Li, Q.; Yang, B.; Lin, H.; Aghdassi, N.; Miao, K.; Zhang, J.; Zhang, H.; Li, Y.; Duhm, S.; Fan, J.; et al. Surface-Controlled Mono/Diselective ortho C–H Bond Activation. *J. Am. Chem. Soc.* **2016**, *138*, 2809–2814. [CrossRef]
47. Zhang, Y.-Q.; Kepčija, N.; Kleinschrodt, M.; Diller, K.; Fischer, S.; Papageorgiou, A.C.; Allegretti, F.; Björk, J.; Klyatskaya, S.; Klappenberger, F.; et al. Homo-coupling of terminal alkynes on a noble metal surface. *Nat. Commun.* **2012**, *3*, 1286. [CrossRef]
48. Eichhorn, J.; Heckl, W.M.; Lackinger, M. On-surface polymerization of 1,4-diethynylbenzene on Cu(111). *Chem. Commun.* **2013**, *49*, 2900–2902. [CrossRef]

49. Fan, Q.; Gottfried, J.M.; Zhu, J. Surface-Catalyzed C–C Covalent Coupling Strategies toward the Synthesis of Low-Dimensional Carbon-Based Nanostructures. *Acc. Chem. Res.* **2015**, *48*, 2484–2494. [CrossRef]
50. Ukah, N.; Wegner, H.A. On-surface synthesis—Ullmann coupling reactions on N-heterocyclic carbene functionalized gold nanoparticles. *Nanoscale* **2024**, *16*, 18524–18533. [CrossRef]

Disclaimer/Publisher's Note: The statements, opinions and data contained in all publications are solely those of the individual author(s) and contributor(s) and not of MDPI and/or the editor(s). MDPI and/or the editor(s) disclaim responsibility for any injury to people or property resulting from any ideas, methods, instructions or products referred to in the content.